Pergamon

Ocean Engineering 28 (2001) 1517–1529

OCEAN ENGINEERING

Wave characteristics past a flexible fishnet

A.T. Chan *, S.W.C. Lee

Department of Mechanical Engineering, The University of Hong Kong, Pokfulam Road, Hong Kong, Hong Kong

Abstract

The scattering of surface waves by a flexible fishnet is studied analytically. The fishnet is modelled as a porous flexible barrier displaced solely by hydrodynamic force like a catenary. The objective is to investigate how a flexible permeable barrier affects the passing waves in the way they are transmitted and reflected, as observed by the fact that the water inside a fishfarm surrounded by fishnets is significantly calmer than that outside. The boundary value problems are solved by defining the reflection coefficient in terms of velocity potential and then the full solutions are obtained by suitable application of the eigenfunction expansion method and the least squares approximation method. The variations of the reflection coefficient, hydrodynamic pressure, barrier deformation and surface wave elevation are determined with respect to the barrier length, porosity and stiffness. It is observed that as the fishnet gets more flexible, its deformation increases and the reflection coefficient decreases, whereas as the fishnet gets more porous, more water can pass through it and thus the reflection coefficient, barrier deformation and the hydrodynamic force are reduced. The flexibility of the barrier behaves like its porosity by allowing more wave energy to act on it through its deformation and hence reduce the reflection and hydrodynamic force of the incident waves acting on the barrier.

Keywords: Flexible porous barrier; Surface waves; Reflection coefficient; Breakwater; Potential flow; Hydrodynamic force; Eigenfunction expansions

1. Introduction

The study of the reflection of harbour waves has been a topic of research interest in fluid mechanics and coastal engineering for a long time (Ursell, 1947). The use of barriers to achieve this end has thus been studied in different problems relating

* Corresponding author. Fax: +852-2858-5415.
E-mail address: atchan@hkucc.hku.hk (A.T. Chan).

0029-8018/01/$ - see front matter
PII: S0029-8018(00)00062-7

to offshore structure designs (Macaskill, 1979). However, in recent decades, porous structures or barriers have been widely used in coastal areas, ever since the analytical development of wave motion past porous media by Sollitt and Cross (1972). Yu and Chwang (1994) studied the wave motion past a two-layered porous structure, while perforated breakwaters were studied by Fugazza and Natale (1992) and Twu and Lin (1991). A comprehensive review on wave motion past porous structures and its engineering applications can be found in Chwang and Chan (1998). Porous breakwater is an ideal choice in breakwater design as it will reduce the hydrodynamic force acting on the structure while preserving the necessary wave reflection.

Apart from the idea of porosity, some engineers may use special materials to build the breakwaters. This novel idea was explored by Wang and Ren (1994) who considered using a flexible plate as a mean to dissipate the wave energy. Inserting the idea of material flexibility into the design of breakwaters also comes from observations in fishfarms. The ponds in the farm are partitioned using fishnets. Obviously, the nets are used in fishfarms with primary consideration to keep the farm under good water circulation. However, it is also observed that the water inside the nets is much calmer than the waters outside. These observed phenomena apparently brought forward the question of the potential application of flexible porous barriers as breakwaters.

We shall consider in this work the effectiveness of the fishnet as a breakwater by studying the scattering of water waves by a flexible porous barrier that extends from the free surface to an arbitrary water depth. Although the scattering of water waves by obstacles has been well documented, the scattering of water waves by vertical porous barriers with mixed boundary conditions has not received much attention in the literature. Macaskill (1979) converted the boundary value problems associated with wave scattering by rigid permeable thin barriers to integro-differential equations. Losada et al. (1992) investigated the scattering of oblique incident waves by rigid barriers in water of finite depth for various configurations of the barrier using the eigenfunction expansion method and the method of least square approximation. This was developed by Sahoo et al. (2000) who extended the study to that of porous barriers. Chwang (1983) developed a porous wavemaker theory based on Darcy's law. Since then, many researchers (see Chwang and Chan, 1998, and references therein) have used Darcy's law to study more general problems of a similar kind. As for flexible barriers, Kim and Kee (1996) and Kee and Kim (1997) studied the wave reflection of horizontal flexible membrane systems. Lo (1998) studied the wave trapping mechanisms of a flexible dual membrane wave barrier.

In the present study, the method of Losada et al. (1992) and Sahoo et al. (2000) is used to study the scattering of incident water waves by a porous flexible fishnet. The fishnet is modelled as a porous, freely flexible barrier that deforms similar to a catenary and its effectiveness as a breakwater is studied in terms of the variation of reflection coefficient against varying membrane length, porosity and flexibility. By application of the eigenfunction expansion method, the problems are converted into dual series relations and the least square approximation is then applied to obtain the reflection coefficients. Other characteristics, such as the hydrodynamic pressure along

the barrier, the membrane deformation and the surface wave amplitude, are also investigated.

2. Mathematical formulation

Under the assumption of the potential theory and linearized theory of surface waves, we study the problem in the two-dimensional Cartesian coordinate system as shown in Fig. 1. The fluid occupies the region $-h \le y \le 0$, $-\infty < x < \infty$ except for the fishnet in the fluid region. The fishnet, assumed thin and light, is located along the y-axis, i.e. $x=0$. The depth of water is h, while the fishnet is submerged at region $-a \le y \le 0$, where a is the length of the fishnet and is always smaller than or equal to h. The barrier is assumed fixed at both ends as in a typical fishfarm arrangement. This is done by mounting the net on frame structures attached near the free surface and anchored with heavy weights. As in Sahoo et al. (2000), we shall use the notation B for barrier and G for the unobstructed gap to denote the region along the line $x=0$.

Assuming the progressive wave which propagates from left to right be represented by

$$\phi = \Re\{\phi_0 \, e^{i(k_0 x - \omega t)} \cosh k_0(y+h)\},$$

with ϕ_0 being the initial velocity potential amplitude and ω the angular frequency of the wave, $k_0 = 2\pi/\lambda$ being the fundamental wave number which satisfies the dispersion relation

$$\omega^2 = g k_0 \tanh k_0 h, \tag{1}$$

g being the gravitational acceleration, and λ the wavelength. Since a part of the wave gets reflected and the other gets transmitted, it suggests the existence of a velocity potential $\Phi[x,y,t]$ of the form $\Phi[x,y,t] = \Re\{\phi_i[x,y] \, e^{-i\omega t}\}$ with $\phi[x,y]$ satisfying the Laplace equation

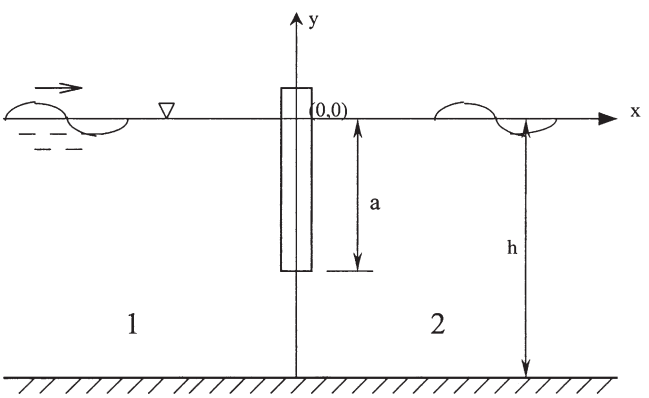

Fig. 1. Schematic diagram of the porous flexible barrier.

$$\left(\frac{\partial^2}{\partial x^2}+\frac{\partial^2}{\partial y^2}\right)\phi_i=0, \text{ in the fluid region} \tag{2}$$

where i=1 and 2 denotes the left and right sides of the barrier respectively, and the linearized free surface boundary condition is,

$$\frac{\partial\phi_i}{\partial y}+K\phi_i=0, \text{ on } y=0, \tag{3}$$

with $K=\omega^2/g$.

The boundary condition on the porous barrier is modified from that given by Chwang (1983) and Wang and Ren (1994), which is based on Darcy's law,

$$\frac{\partial\phi_i}{\partial x}=ik_0G(\phi_1-\phi_2)-i\omega s \text{ on } x=0,\ -a\le y\le 0 \tag{4}$$

where G is the porous-effect parameter defined by Chwang (1983). $s=s[y]\,e^{-i\omega t}$ is the fishnet displacement defined by its own dynamical equation given by Lo (1998)

$$\frac{d^2s}{dy^2}=-\frac{i\omega}{D}(\phi_1-\phi_2)=\frac{i\omega}{D}\phi[y] \tag{5}$$

where D is the normalized stiffness of the barrier and is related to the tension of the net F by

$$D=F\cos\theta \tag{6}$$

θ is the angle of the fishnet deformation with respect to the y-axis, assuming that the deformation of the fishnet remains small.

The continuity of velocity and pressure along the gap is given by

$$\phi_i,\ \frac{\partial\phi_i}{\partial x} \text{ continuous on } x=0,\ -a\le y\le 0. \tag{7}$$

The radiation and bottom boundary conditions are of the form

$$\phi_1[x,y]=\frac{\phi_0\cosh k_0(y+h)}{\cosh k_0h}(e^{ik_0x}+R_0\,e^{-ik_0x}) \text{ as } x\to-\infty, \tag{8}$$

$$\phi_2[x,y]=\frac{T_0\phi_0\cosh k_0(y+h)}{\cosh k_0h}\,e^{ik_0x} \text{ as } x\to\infty, \tag{9}$$

and

$$\frac{\partial\phi}{\partial y}=0, \text{ on } y=-h, \tag{10}$$

where R_0 and T_0 are the unknown reflection and transmission coefficients to be determined.

3. Method of solutions

For the region left of the barrier, the velocity potential $\phi_1[x,y]$ satisfying Eq. (2) and boundary conditions (3), (9) and (10) can be written as

$$\phi_1[x,y]=\frac{\phi_0 \cosh k_0(y+h)}{\cosh k_0 h}(e^{ik_0x}+R_0\, e^{-ik_0x})+\sum_{n=1}^{\infty}\frac{\phi_0 R_n\, e^{k_nx}\cos k_n(y+h)}{\cos k_n h},\ x<0, \tag{11}$$

and the transmitted wave is

$$\phi_2[x,y]=\frac{\phi_0 T_0 \cosh k_0(y+h)\, e^{ik_0x}}{\cosh k_0 h}+\sum_{n=1}^{\infty}\frac{\phi_0 T_n\, e^{-k_nx}\cos k_n(y+h)}{\cos k_n h},\ x\geq 0, \tag{12}$$

where R_n and T_n (n=1,2,...) are reflection and transmission coefficients corresponding to the evanescent wave modes in regions 1 and 2 respectively. The wave numbers k_n satisfy the dispersion relations for evanescent wave modes,

$$\omega^2+gk_n \tan k_n h=0 \text{ for } n=1,2,... \tag{13}$$

From the condition that the velocity and pressure, i.e. $[(\partial\phi_i)/(\partial x)]$ and ϕ_i, are continuous along the line x=0, $-h\leq y\leq 0$, we can derive that

$$\phi_1=\phi_2,\ \frac{\partial\phi_1}{\partial x}=\frac{\partial\phi_2}{\partial x}\ x=0,\ -h\leq y\leq -a \tag{14}$$

which in terms of reflection and transmission coefficients

$$R_0+T_0=1,\ R_n+T_n=0, \text{ for } n=1,2,\ldots \tag{15}$$

Upon substituting Eq. (15) into the wave potential functions $\phi_1[x,y]$ and $\phi_2[x,y]$, we have

$$\phi_1[x,y]=\frac{\phi_0 \cosh k_0(y+h)}{\cosh k_0 h}(e^{ik_0x}+R_0\, e^{-ik_0x})+\sum_{n=1}^{\infty}\frac{\phi_0 R_n\, e^{k_nx}\cos k_n(y+h)}{\cos k_n h},\ x<0, \tag{16}$$

$$\phi_2[x,y]=\frac{\phi_0(1-R_0) \cosh k_0(y+h)\, e^{ik_0x}}{\cosh k_0 h}-\sum_{n=1}^{\infty}\frac{\phi_0 R_n\, e^{-k_nx}\cos k_n(y+h)}{\cos k_n h},\ x\geq 0, \tag{17}$$

Along the line x=0, we define the pressure potential ϕ_p,

$$\phi_p=\phi_1-\phi_2=\left(2\frac{R_0 \cosh k_0(y+h)}{\cosh k_0 h}+2\sum_{n=1}^{\infty}\frac{R_n \cos k_n(y+h)}{\cos k_n h}\right)\phi_0 \text{ at } x=0. \tag{18}$$

And putting ϕ into Eq. (5) and integrating, we obtain

$$s=\left(2\left(\frac{R_0 \cosh k_0(y+h)}{k_0^2 \cosh k_0 h}-\sum_{n=1}^{\infty}\frac{R_n \cos k_n(y+h)}{k_n^2 \cos k_n h}\right)+B_1y+B_0\right)\frac{i\omega\phi_0}{D} \tag{19}$$

with the integrating constants B_0 and B_1 to be found later. Using Eqs. (19) and (4), for the barrier region we get,

$$-\frac{ik_0\cosh k_0(y+h)}{\cosh k_0 h}+\frac{iR_0\cosh k_0(y+h)}{\cosh k_0 h}\left(k_0+2\left(G-\frac{i\omega^2}{Dk_0^2}\right)\right) \tag{20}$$

$$-\sum_{n=1}^{\infty}\frac{R_n\cos k_n(y+h)}{\cos k_n h}\left(k_n-2i\left(G+\frac{i\omega^2}{Dk_n^2}\right)\right)+\frac{\omega^2}{D}(B_1y+B_0)=0,\ \text{for } -a\le y\le 0.$$

Using Eq. (14), we have in the gap region,

$$\frac{R_0\cosh k_0(y+h)}{\cosh k_0 h}+\sum_{n=1}^{\infty}\frac{R_n\cos k_n(y+h)}{\cos k_n h}=0 \text{ for } -h\le y\le -a. \tag{21}$$

Considering that the fishnet is fixed at both ends, that is

$$s[-a]=s[0]=0, \tag{22}$$

we can solve for B_0 and B_1 giving,

$$B_0=2\sum_{n=1}^{\infty}\frac{R_n}{k_n^2}-\frac{2R_0}{k_0^2} \tag{23}$$

$$B_1=\frac{1}{a}\left(2\sum_{n=1}^{\infty}\frac{R_n}{k_n^2}-\frac{2R_0}{k_0^2}+2\sum_{n=1}^{\infty}\frac{R_n\cos k_n(h-a)}{k_n^2\cos k_n h}-\frac{R_0\cosh k_0(h-a)}{k_0^2\cosh k_0 h}\right) \tag{24}$$

Let us define

$$H[y] \tag{25}$$

$$=\begin{cases}-\dfrac{ik_0\cosh k_0(y+h)}{\cosh k_0 h}+\dfrac{iR_0\cosh k_0(y+h)}{\cosh k_0 h}\left(k_0+2\left(G-\dfrac{i\omega^2}{Dk_0^2}\right)\right) & \\ -\displaystyle\sum_{n=1}^{\infty}\frac{R_n\cos k_n(y+h)}{\cos k_n h}\left(k_n-2i\left(G+\frac{i\omega^2}{Dk_n^2}\right)\right) & \\ +\dfrac{\omega^2}{D}(B_1y+B_0), & \text{for } -a\le y\le 0\\ \dfrac{R_0\cosh k_0(y+h)}{\cosh k_0 h}+\displaystyle\sum_{n=1}^{\infty}\frac{R_n\cos k_n(y+h)}{\cos k_n h}, & \text{for } -h\le y\le -a\end{cases}$$

By application of the least-square method, we enforce

$$\int_{-h}^{0}H^*[y]\frac{\partial H[y]}{\partial R_n}\,dy=0 \text{ for } n=0,1,\ldots \tag{26}$$

with the asterisk denoting the complex conjugate with

$$H^*[y]=R_0^*f_0^*[y]+\sum_{n=1}^{\infty}R_n^*f^*[y]+h_n^*[y]. \tag{27}$$

To perform the integral (26), we need to find the respective derivatives. Thus

$$\left.\begin{aligned}&\frac{\partial H}{\partial R_0}=\frac{i\cosh k_0(y+h)}{\cosh k_0h}\left(k_0+2\left(G-\frac{i\omega^2}{Dk_0^2}\right)\right)=f_0[y]\\&\frac{\partial H}{\partial R_n}=-\left(k_n-2i\left(G+\frac{i\omega^2}{Dk_n^2}\right)\right)\frac{\cos k_n(y+h)}{\cos k_nh}=f_n[y]\\&h[y]=-i\left(\frac{k_0\cosh k_0(y+h)}{\cosh k_0h}+\frac{i\omega^2}{D}(B_1y+B_0)\right)\end{aligned}\right\}\ \text{Barrier: } -a\le y\le 0 \tag{28}$$

$$\left.\begin{aligned}&\frac{\partial H}{\partial R_0}=\frac{\cosh k_0(y+h)}{\cosh k_0h}=f_0[y]\\&\frac{\partial H}{\partial R_n}=\frac{\cos k_n(y+h)}{\cos k_nh}=f_n[y]\\&h[y]=0\end{aligned}\right\}\ \text{Gap: } -h\le y\le -a \tag{29}$$

On substituting Eq. (29) into Eq. (26) and upon truncation to a finite number of terms N, we derive that

$$\sum_{m=0}^{N}R_m^*X_{m,n}=b_n\ n=0,1,\ldots,N \tag{30}$$

which is an $(N+1)\times(N+1)$ system of linear equations for the determination of the reflection coefficients R_n^* with,

$$\begin{aligned}&X_{00}=\int_{-h}^{0}f_0^*f_0\,\mathrm{d}y,\quad X_{m0}=\int_{-h}^{0}f_m^*f_0\,\mathrm{d}y\\&X_{mn}=\int_{-h}^{0}f_m^*f_n\,\mathrm{d}y,\quad b_n=-\int_{-h}^{0}h^*f_n\,\mathrm{d}y\ \text{for } m,n=0,1,\ldots,N\end{aligned} \tag{31}$$

where the integration $\int_{-h}^{0}$ implies $\int_{-h}^{-a}+\int_{-a}^{0}$, or $\int_G+\int_B$.

4. Numerical results and discussions

From Eq. (30) a complex system of equations is obtained which when solved will give the reflection coefficients. The advantages of this eigenfunction expansion combined with the least-squares method are its ability to tackle many problems of a similar nature to the aforementioned configurations and its efficiency (Sahoo et

al., 2000). In a preliminary trial test for convergence, it is found that 5 to 10 terms are sufficient for the determination of the reflection coefficients $|R_0|$ to an accuracy of five decimal places for all cases under study. In this study, we used N=9 for uniformity.

We first investigate the variation of reflection coefficient with respect to different fishnet length and stiffness. Fig. 2 shows the variation of the reflection coefficient against the normalized membrane length (a/h) for different values of D for the porous-effect parameter G=1 and the wave-effect parameter C=1. The wave-effect parameter C is defined by Chwang (1983) as

$$C=\frac{g}{\omega^2 h}, \tag{32}$$

which is a comparison between gravitational effect and oscillation effect. From the figure it can be seen that the reflection coefficient increases generally with respect to increasing barrier length, although the increase is very slow. This is expected, as the longer the barrier, the more blockage it handles, and therefore the reflection coefficient increases. In fact as the non-dimensional length reaches 0.1, the increase in the reflection coefficient almost stagnates. Only when the length increases further to 0.9 does a more noticeable increase begin to occur. From this it can be seen that the use of a very long barrier is not economical as the surface wave energy is concentrated in the free surface and thus the lower part of the barrier plays only a small role in wave reflection. The apparent low dependence on the draft of the barrier is also partially explained by the relative high porosity in the study case. It is also observed that the more flexible the fishnet, the smaller the reflection coefficient. This is because as D increases, the barrier becomes stiffer and more rigid and thus it reflects more wave energy. For stiffness larger than 1, the reflection coefficient

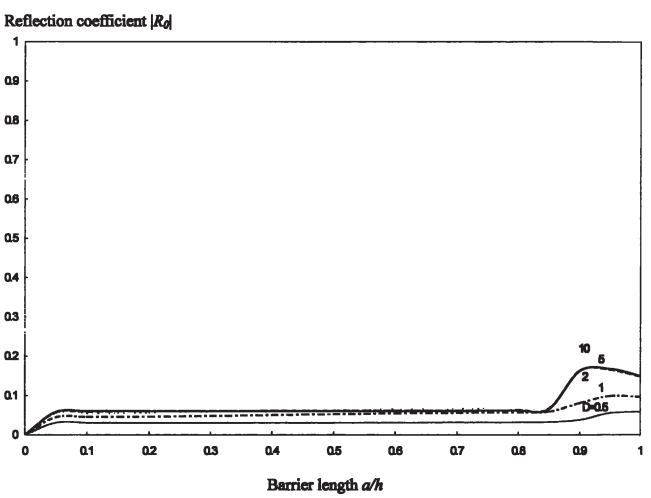

Fig. 2. Variation of reflection coefficient $|R_0|$ against normalized barrier length a/h for various values of barrier stiffness D; C=G=1.

changes slightly with stiffness except for the larger barrier length when the barrier suffers more significant deformation. Our solutions are in agreement with the previous results obtained by Sahoo et al. (2000) for rigid barriers.

Fig. 3 shows the variation in the reflection coefficient with the barrier length for different values of the porous-effect parameter G with stiffness parameter D=1. Again the reflection coefficient increases with the dimensionless barrier length a/h for reasons similar to those given for Fig. 2. Also except for the case when G=0, the increase in the reflection coefficient is only significant from a/h=0 to 0.1, which is again because of the wave energy concentration at the free surface. It can also be seen that the reflection coefficient decreases with increasing G for fixed a/h. This also agrees with physical intuition because larger G (larger permeability) allows more fluid and thus more energy to pass through. In the limit, when G=0 corresponding to an impermeable barrier and a/h=1, all energy is being reflected and thus $|R_0|$=1, meaning a total partitioning of the fluid domain. The results agree with that obtained in the limiting case of a single impermeable membrane described by Lo (1998). We also include in the graph the cases when G is complex, meaning that the porosity also contains a resistive component. A resistive component of the porosity produces more friction and makes the barrier more difficult to penetrate and hence more solid. The result is larger reflection coefficient, as discussed by Yu and Chwang (1994) and Chan et al. (1999).

Fig. 4 shows the variation of the reflection coefficient versus the wave-effect parameter C for various values of barrier stiffness with fixed barrier length a/h=0.5 and porous effect parameter G=1. We can see from the graph that as the wave-effect parameter C is small, the reflection coefficient is back to nearly 1. This agrees with the results of Losada et al. (1992) and Sahoo et al. (2000). For small C, transmission is enhanced by the slowness of oscillation due to uniform behaviour of the potential far from the barrier (Tuck, 1975); when C is small, gravitational force is dominant, and thus the propagation of the wave energy is restrained and retarded. This can

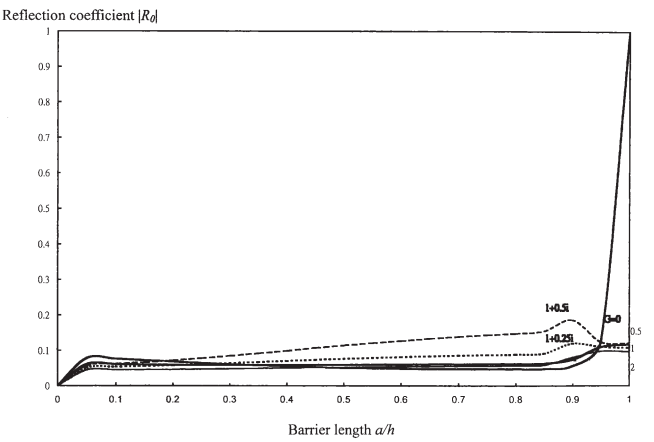

Fig. 3. Variation of reflection coefficient $|R_0|$ against normalized barrier length a/h for various values of barrier porosity G; C=D=1.

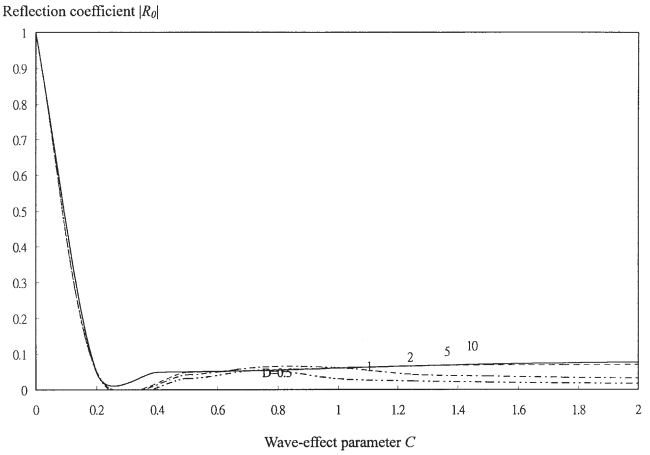

Fig. 4. Variation of reflection coefficient $|R_0|$ against wave-effect parameter C for various values of barrier stiffness D, G=1 and normalized barrier length a/h=0.5.

also be interpreted that short waves are more reflected than long waves as in Yu and Chwang (1994). Increasing the barrier stiffness also shows a minor increase in the wave reflection with explanation similar to that given above.

Fig. 5 shows the variation of the hydrodynamic pressure acting on the permeable flexible fishnet against the vertical distance y/h for different values of membrane stiffness for barrier length a/h=0.5, porosity factor G=1 and wave-effect parameter C=1. We define the normalized pressure force p as $(\phi_1[0,y]-\phi_2[0,y])/(\sqrt{C}\phi_0)$. A finite value of force is assumed at the tip of the barrier so that the pressure force only exists for the barrier region but not in the open region. It can be observed that the hydrodynamic force generally increases with increasing stiffness. This is expected

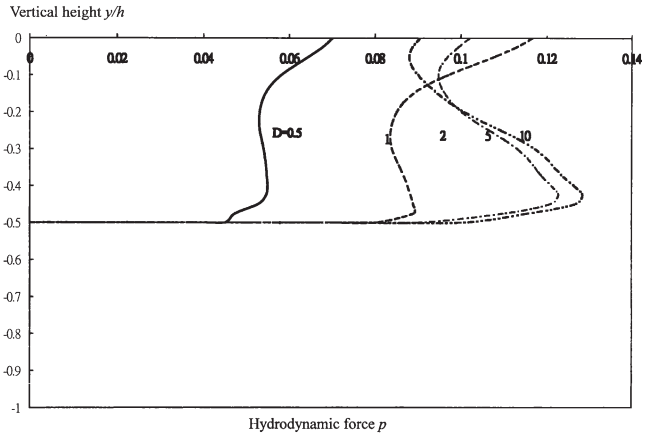

Fig. 5. Variation of hydrodynamic force p against the vertical height y/h for various values of barrier stiffness D, C=G=1, a/h=0.5.

as a more rigid barrier will tend to react to more wave action and thus a larger force is experienced. On the other hand, a more flexible barrier will simply deform with respect to the force. Also for large value of stiffness D, the hydrodynamic pressure p increases with depth. However, as the value of stiffness decreases, the sign of the variation starts to change drastically. The pressure force exhibits some form of 'instability' at $D\approx 2.5$, where it changes from an increasing function to a decreasing one once it attains the threshold. This is due to the cosh $k_0 y$ term, which becomes increasingly dominant compared to the evanescent wave mode with the variation of stiffness. The variation of sign of the pressure gradient is also a result of wave energy distribution due to partial reflection of the fishnet, and it obviously depends on the amount of energy partitioned by the barrier.

Fig. 6 shows the normalized membrane deformation s/h with respect to various values of the barrier stiffness for $C=G=1$ and normalized length $a/h=0.5$. Obviously as the membrane stiffness increases, the deformation becomes smaller. The barrier bulges more at the lower end of the barrier, which corresponding to the hydrodynamic force distribution. Fig. 7 shows the respective barrier deformation under various values of the porous-effect parameter G for normalized stiffness $D=1$. Basically, for real values of G, increasing porosity decreases barrier deformation. This is because when the porosity is small, the barrier is being imparted with more energy and thus it results in a larger deformation. When G is complex, the imaginary part, which represents the frictional part of the porosity, will act as an extra barrier to block wave energy. With more blockage, the resulting hydrodynamic force becomes larger and thus the membrane deformation increases with the increasing imaginary part of the porous-effect parameter.

The normalized free surface profile η/h for various values of stiffness D for $C=G=1$ is plotted as in Fig. 8. It is observed that increasing stiffness not only decreases wave amplitude but a phase shift whose magnitude is proportional to the stiffness is also produced. A minor wave pile-up characteristic of wavemaking is

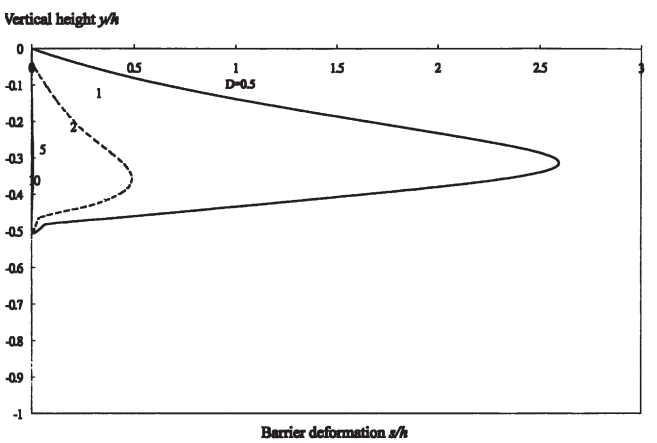

Fig. 6. Variation of barrier deformation s/h against the vertical height y/h for various values of barrier stiffness D, $C=G=1$, $a/h=0.5$.

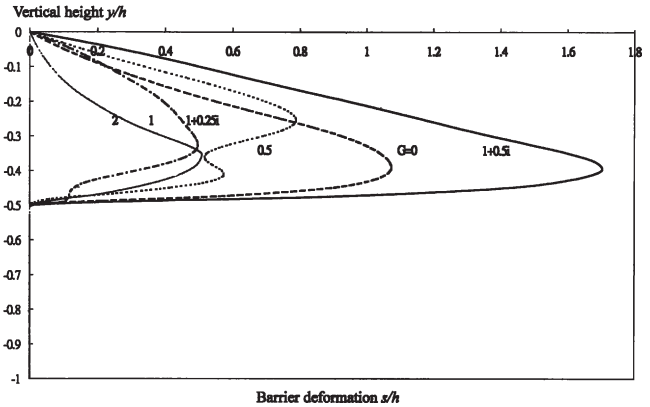

Fig. 7. Variation of barrier deformation s/h against the vertical height y/h for various values of the porous-effect parameter G, C=D=1, a/h=0.5.

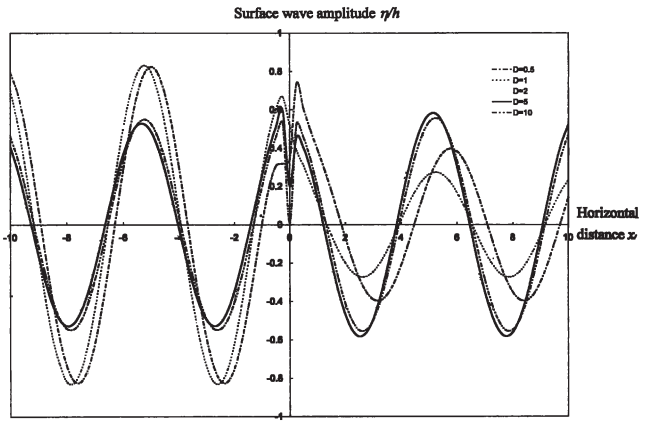

Fig. 8. Surface wave amplitude η/h against distance x/h for various values of the barrier stiffness D, C=G=1, a/h=0.5.

also observed at the barrier tip. Both of these are produced by the coupled motion of the barrier deformation.

5. Conclusions

The wave scattering of a flexible permeable fishnet is investigated in this paper. The reflection coefficients, barrier deformation, hydrodynamic force and surface wave are investigated for various values of barrier stiffness D, barrier length a/h, wave-effect parameter C and porous-effect parameter G. As the stiffness of the fishnet increases, the deformation of the net decreases which results in an increase in reflection coefficient and hydrodynamic force. The present work represents a prelimi-

nary step in the study of the use of a flexible permeable barrier as a breakwater. It shows the effectiveness and possible use of a fishnet in wave reflection and seems to provide an economical and feasible alternative to a rigid impermeable breakwater. Further work along this direction will be carried out in the future.

Acknowledgements

The authors thank Dr T. Sahoo for discussions and comments on this work. This research work was sponsored partially by The University of Hong Kong under the Area of Excellence Grant.

References

Chan, A.T., Sahoo, T., Chwang, A.T., 1999. Reflection of water waves by sloping porous structures. In: Proceedings of the Ninth International Offshore and Polar Engineering Conference, vol. 3., pp. 743–748.

Chwang, A.T., 1983. A porous wavemaker theory. Journal of Fluid Mechanics 132, 395–406.

Chwang, A.T., Chan, A.T., 1998. Interaction between porous media and wave motion. Annual Review of Fluid Mechanics 30, 53–84.

Fugazza, M., Natale, L., 1992. Hydraulic design of perforated breakwaters. Journal of Waterway, Port, Coastal and Ocean Engineering 115 (1), 1–14.

Kee, S.T., Kim, M.H., 1997. Flexible membrane wave barrier II: Floating/submerged buoy–membrane system. Journal of Waterway, Port, Coastal and Ocean Engineering 123 (2), 82–90.

Kim, M.H., Kee, S.T., 1996. Flexible membrane wave barrier I: Analytical and numerical solutions. Journal of Waterway, Port, Coastal and Ocean Engineering 122 (1), 46–53.

Lo, E.Y.M., 1998. Flexible dual membrane wave barrier. Journal of Engineering Mechanics 124 (5), 264–271.

Losada, I.J., Losada, M.A., Roldan, A.J., 1992. Propagation of oblique incident waves past rigid vertical thin barriers. Applied Ocean Research 14, 191–199.

Macaskill, C.C., 1979. Reflexion of water waves by permeable barriers. Journal of Fluid Mechanics 95, 141–157.

Sahoo, T., Chan, A.T., Chwang, A.T., 2000. Scattering of oblique surface waves by permeable barriers. Journal of Waterway. Port, Coastal and Ocean Engineering 126 (4), 196–205.

Sollitt, C.K., Cross, R.H., 1972. Wave transmission through permeable breakwaters. In: Proceedings of the Thirteenth Coastal Engineering Conference, pp. 1827–1846.

Tuck, E.O., 1975. Matching problems involving flows through small holes. Advances in Applied Mechanics 15, 89–157.

Twu, S.W., Lin, D.T., 1991. On a highly effective wave absorber. Coastal Engineering 15, 389–405.

Ursell, F., 1947. The effect of a fixed vertical barrier on surface waves in deep water. Proceedings of the Cambridge Philosophical Society 43, 374–382.

Wang, K.H., Ren, X., 1994. An effective wave trapping system. Ocean Engineering 21 (2), 155–178.

Yu, X., Chwang, A.T., 1994. Wave motion through porous structures. Journal of Engineering Mechanics 120 (5), 989–1008.